Plant invasions and extinction debts

Benjamin Gilbert[a,b,1] and Jonathan M. Levine[b,c]

[a]Department of Ecology and Evolutionary Biology, University of Toronto, Toronto, ON, Canada M5S 3B2; [b]Department of Ecology, Evolution, and Marine Biology, University of California, Santa Barbara, CA 93106; and [c]Institute for Integrative Biology, Eidgenössiche Technische Hochschule Zurich, 8092 Zurich, Switzerland

Edited by Monica G. Turner, University of Wisconsin-Madison, Madison, WI, and approved November 28, 2012 (received for review July 20, 2012)

Whether introduced species invasions pose a major threat to biodiversity is hotly debated. Much of this debate is fueled by recent findings that competition from introduced organisms has driven remarkably few plant species to extinction. Instead, native plant species in invaded ecosystems are often found in refugia: patchy, marginal habitats unsuitable to their nonnative competitors. However, whether the colonization and extinction dynamics of these refugia allow long-term native persistence is uncertain. Of particular concern is the possibility that invasive plants may induce an extinction debt in the native flora, where persistence over the short term masks deterministic extinction trajectories. We examined how invader impacts on landscape structure influence native plant persistence by combining recently developed quantitative techniques for evaluating metapopulation persistence with field measurements of an invaded plant community. We found that European grass invasion of an edaphically heterogeneous California landscape has greatly decreased the likelihood of the persistence of native metapopulations. It does so via two main pathways: (*i*) decreasing the size of native refugia, which reduces seed production and increases local extinction, and (*ii*) eroding the dispersal permeability of the matrix between refugia, which reduces their connectivity. Even when native plant extinction is the deterministic outcome of invasion, the time to extinction can be on the order of hundreds of years. We conclude that the relatively short time since invasion in many parts of the world is insufficient to observe the full impact of plant invasions on native biodiversity.

metacommunity | metapopulation | invasive species | spatial ecology | temporal lag

Introduced species are often considered a leading threat to native biodiversity (1, 2). However, recent syntheses show that competition from introduced species, and plant invaders in particular, has only rarely resulted in extinction (3–6). This trend has emerged because, in the short term at least, invasive plants do not completely extirpate native plant species but rather reduce their distribution and abundance, often restricting them to isolated habitat refugia (7–9). Despite well-established cases of native plants occupying distinct refugia and outperforming invasive plant species in those habitats (8, 10, 11), the long-term dynamics of native species in these refugia are poorly understood. Given the global prevalence of plant displacement by invasions, it is important to develop a general method for predicting how extinction debts may develop following invasions.

The metapopulation framework, which considers a network of isolated populations connected via dispersal, provides an excellent starting point for understanding the long-term consequences of invasions. When native populations are relegated to spatially isolated refugia, their long-term persistence is regulated by the colonization and extinction dynamics in their entire metapopulation (12). A large body of work suggests that even a partial loss of habitat in metapopulations, such as might arise from invasion, can deterministically drive the system to extinction (13, 14). However, due to slow colonization and extinction dynamics, this outcome often occurs many generations after habitat loss, generating an extinction debt in the meantime (15–17).

General metapopulation models indicate that reductions in colonization rates or increases in extinction rates reduce the viability of the metapopulation, and may therefore lead to an extinction debt (18). However, these models have yet to incorporate the mechanistic links between the local impacts of invasive species and the global persistence of the metapopulation. This prevents us from understanding the relative importance of different types of invader impacts on native persistence, and which native species will be most sensitive to these impacts at the metapopulation scale. In this study, we first present a theoretical model for understanding how extinction debts arise in invaded landscapes. We then parameterize and apply this model to understand the potential for invasive plant impacts on native annual plant persistence in a spatially heterogeneous serpentine soil landscape in California. Invasions are widespread in these landscapes, and they have likely reduced the connectivity and extent of local native patches within the broader metapopulation (9, 19). Serpentine landscapes support a disproportionate number of rare and threatened plant species, and therefore have a high conservation value (20). We show that invader impacts on the size and/or quality of native refugia and the permeability of the matrix between refugia can greatly reduce native plant metapopulation persistence and force extinction hundreds of years after the invasion is complete.

Model Framework and Application to the Focal System

Our modeling framework builds on recent advances in metapopulation theory (13, 14) to quantify and partition invader impacts on the viability of native metapopulations in real landscapes. We assume that as invasions increasingly relegate native species to isolated patches (7, 9, 19), they can generate extinction debts via two main impacts (Fig. 1*A*): effects on patch size and effects on the dispersal permeability of the habitat matrix between patches. Reducing patch size reduces the number of seed-producing individuals, and thereby depresses the colonization probability in the metapopulation (Fig. 1*A*, arrow a). This impact is particularly severe when the invader eliminates the most favorable habitat. Reducing patch size also hinders colonization by making patches effectively further from one another (Fig. 1*A*, arrow b) and increases the stochastic extinction rate by reducing the number of individuals in a patch (Fig. 1*A*, arrow c).

The second pathway of impact occurs when the invader alters the dispersal permeability of the matrix between suitable patches (Fig. 1*A*, arrow d). Although the matrix may not support stable populations, it may support transient sink populations. These sinks may provide critical intermediate steps for dispersal between patches by allowing many incoming seeds to produce a few plants whose seeds may then disperse onward in the next generation. Many plant species have extremely limited dispersal (9, 21); thus, this "multigenerational dispersal" can help overcome dispersal limitation.

To model these processes, we begin with methods developed by Hanski and Ovaskainen (13, 14) to analyze spatially explicit metapopulations with dynamics in discrete time. In what follows, we first describe the model and then show how one can obtain

Author contributions: B.G. and J.M.L. designed research; B.G. performed research; B.G. analyzed data; and B.G. and J.M.L. wrote the paper.

The authors declare no conflict of interest.

This article is a PNAS Direct Submission.

Freely available online through the PNAS open access option.

[1]To whom correspondence should be addressed. E-mail: benjamin.gilbert@utoronto.ca.

This article contains supporting information online at www.pnas.org/lookup/suppl/doi:10.1073/pnas.1212375110/-/DCSupplemental.

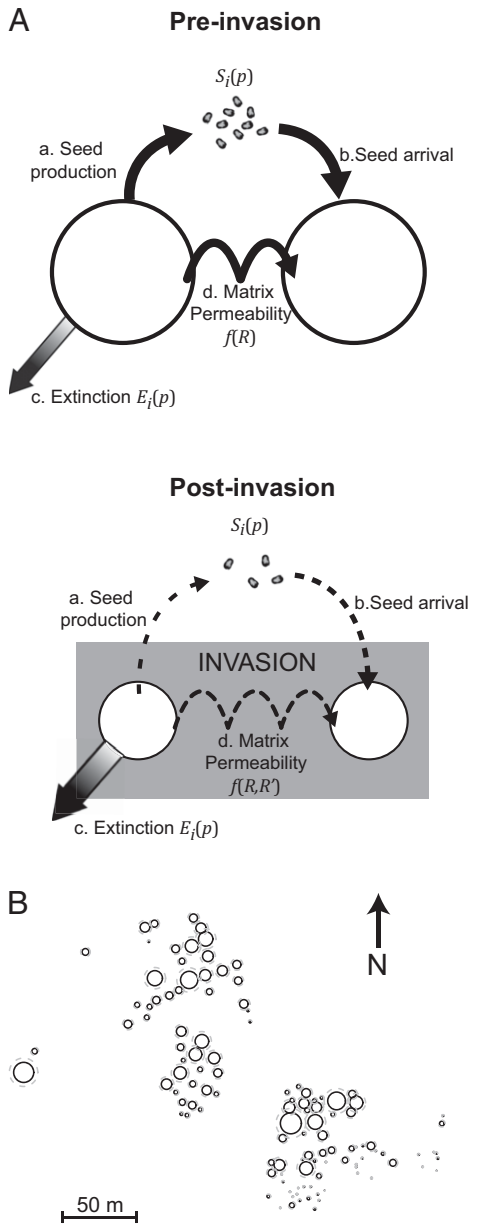

Fig. 1. Metapopulation viability in the study system following invasion. (*A*) Metapopulation dynamics preinvasion and postinvasion, with the width of arrows signifying the strength of the process. Invaders reduce colonization rates through decreased seed production and by altering competitor composition between patches (matrix permeability). Reduced local population sizes also increase local extinction rates. (*B*) Spatial layout of the study system. Black lines represent present-day distributions, and dashed gray lines represent one preinvasion scenario in which the habitat of native annuals was double the present-day area.

mathematical expressions for metapopulation persistence with this model structure. Next, we show how these expressions can be modified to incorporate the different ways invaders might affect native metapopulations (Fig. 1) and how their influence on metapopulation persistence can be numerically evaluated. We then apply these techniques to our field system to determine the impacts of invaders on the metapopulation dynamics of several focal species. Finally, we use simulations of the model to estimate times to extinction.

Consider a vector of patch occupancy probabilities, where each element corresponds to a specific patch in the metapopulation. The change in a species' probability of occurrence (p) in patch i is the difference between the probability of patch colonization (C_i) and its probability of extinction (E_i):

$$\Delta p_i = C_i(p)(1-p_i) - E_i(p)(p_i). \quad [1A]$$

We model the colonization probability as a Monod function that approaches one with high seed arrival from other patches [$S_i(p)$]:

$$C_i(p) = \frac{S_i(p)}{S_i(p)+\frac{1}{c}}, \text{where } S_i(p) = \sum_{j\neq i} \mu A_j p_j K_{ij}. \quad [1B]$$

Seed arrival to patch i is the sum of the contributions from all occupied patches j ($p_j = 1$). The contribution of each occupied patch j is the product of the number of seeds produced (seeds produced per unit area, μ, multiplied by patch area (A_j) and the probability of dispersing from patch j to i. This dispersal probability is defined by the dispersal kernel (K_{ij}), which is a function of the distance between patches and other metapopulation characteristics described below. The parameter c regulates how rapidly the probability of colonization increases with seed arrival.

We assume that the extinction probability, $E_i(p)$, is inversely related to the size of the population in a patch:

$$E_i(p) = eD_i(1-C_i(p)), \text{ where } D_i = (1/\mu A_i). \quad [1C]$$

Specifically, the extinction rate is the product of e, the extinction probability for a patch with a single individual; D_i, the inverse of patch population size; and $(1-C_i(p))$, the probability the patch is not immediately recolonized (a rescue effect).

Returning to the colonization rate, the connectivity of the metapopulation is determined by the dispersal kernel, K_{ij}, which is influenced by the distance between patches (d_{ij}), the size of the recipient patch (the "target area"; Fig. S1), mean dispersal distance (σ), and the matrix permeability, measured as the annual plant's finite rate of increase in the matrix (R; Fig. 1*A*, arrow d). Because species in our system can make seeds in the matrix habitat but not enough to replace themselves ($0 < R < 1$), some colonization of other patches might arise from multigenerational spread through the matrix. We therefore model dispersal as a random walk allowing a focal seed produced in patch j to disperse directly to patch i or to make offspring that land in the matrix but eventually disperse to patch i. Each step in the walk, apart from the initial dispersal from patch j, is taken with probability R [the average number of offspring per seed in the matrix (<1)]. The kernel that defines the per-seed probability of dispersing to focal patch i in exactly n generations (Q_n) can then be expressed (*SI Materials and Methods*, *Dispersal function*):

$$Q_n = R^{n-1}k\frac{1}{\sqrt{n}}\frac{\sqrt{A_i}}{\sigma d_{ij}}\int\left(\exp\left(-x^2/2\left(\sqrt{n}\sigma\right)^2\right)\right)dx\ (1-Q_{n-1}), \quad [2]$$

where k is a normalization constant and the integral is evaluated over the range of $d_{ij} \pm radius_i$. The probability of dispersing, K_{ij}, in any number of generations (1 to ∞) becomes $\sum_{n=1}^{\infty} Q_n$.

Having specified the model, we follow the approach of Hanski and Ovaskainen (13, 14) to analyze metapopulation persistence, the ability to recover from a drop to low patch occupancy. Doing so requires first defining a function g that describes the expected contribution of a patch to metapopulation persistence. Defined as the colonization probability (Eq. **1*B***) divided by the extinction probability (Eq. **1*C***) for patch i, g_i is somewhat analogous to a local growth rate that results from the colonization and persistence of immigrants from other patches in the metapopulation. We then build a (mathematical) matrix **M**, where each element (m_{ij}) is the partial derivative $\partial g_i(p)/\partial p_j$ evaluated at $P = 0$, in other words, how metapopulation "growth" from a low probability of occupancy in patch i changes with occupancy in patch j. For our model (Eq. **1**), calculation of this partial derivative generates elements m_{ij} equal those of the spatially explicit Levins model (13, 14):

ECOLOGY

$$m_{ij} = {c\mu A_j K_{ij}}\Big/{eD_i} \text{ and diagonal elements } m_{ii} = 0. \quad [3]$$

To persist, the metapopulation must show increasing occupancy when occupancy drops to very low levels. This persistence criterion is met when the leading eigenvalue (λ) of **M** is greater than 1 (13, 14).

Having specified the persistence criteria for the metapopulation, we can now model how invasion effects on different parameters in the colonization and extinction functions (the various arrows in Fig. 1*A*) have an impact on metapopulation persistence. Specifically, we consider the effects of reduced refugia area, lowered seed density when invasion removes the most favorable habitat, and reduced dispersal permeability of the grassland matrix between refugia. When these three changes are incorporated into the colonization and extinction functions, and substituted into Eq. **3**, the off-diagonal elements in **M** become:

$$m_{ij} = \frac{c}{e}\mu^2 A_i A_j (w' H_F)^2 f\left(d_{ij}, R, R', A_i, H_F, \sigma\right). \quad [4]$$

Here, H_F is the fraction of habitat remaining after invasion, A signifies the preinvasion patch area, and w' is the seed density after invasion divided by before invasion (Table S1). R is the finite rate of increase in the matrix before invasion, and R' is the R after invasion divided by before invasion (Table S2). Importantly, Eq. **4** can be partitioned into two multiplicative components: The first half incorporates the effect of invasion on native persistence through its impact on seed production, and the second half (the function f, which is the kernel K_{ij} following invasion) incorporates its impact on connectivity.

After incorporating these invader impacts, native plant persistence in the metapopulation is predicted when $\lambda_{postinvasion} > 1$. Empirically estimating λ, and thus predicting extinction debts, is challenging because the presence of an extinction debt precludes standard estimation techniques for metapopulations at equilibrium (12, 22), and several of the parameters required to parameterize λ accurately are difficult to attain precisely for most species. However, the criteria for metapopulation persistence can be expressed in terms of the ratio of λ's preinvasion and postinvasion. This ratio does not depend on some of the parameters that are more difficult to measure (e.g., c, e), and it provides a continuous measure of the contribution of invasion to reduced persistence. A metapopulation enters an extinction debt when:

$$\lambda_{post-inv}\Big/\lambda_{pre-inv} < 1 - p^*_{pre-inv}. \quad [5]$$

Combined with the determinants of λ in invaded and uninvaded systems (Eqs. **3** and **4**), the ratio in Eq. **5** allows empiricists to scale the local impacts of invasion on patch size and matrix permeability to the expected proportional change in metapopulation persistence (λ) (the mathematics are presented in *SI Materials and Methods, Incorporating invasion into the model*). Whether this change is enough to force eventual extinction depends on the species' spatially weighted patch occupancy before invasion, $p^*_{pre-inv}$. Although our lack of knowledge of this value ultimately prevents us from identifying which species suffer from extinction debts, we can use the left-hand side of Eq. **5** to predict the impact of invasions on the degree to which metapopulations are buffered from extinction.

We used the model to predict the impacts of invasion on metapopulation persistence in an edaphically heterogeneous California landscape. The habitat is derived from serpentine parent material but is topographically heterogeneous, with rocky hummocks interspersed by more finely textured clay soils. Native annual forbs and native perennial grasses dominated this area before European annual grass invasion (9, 23, 24), but the forbs now occur on small rocky refugia, surrounded by a matrix of exotic grasses (8, 9, 19) (Fig. 1*B*). Species in similar habitats have previously been shown to exhibit colonization and extinction dynamics typical of metapopulations (25, 26), and native species' distributions in our study area are consistent with predictions for metapopulations (Fig. S2).

To demonstrate that invasion has definitely driven extinction debts in a native community, one requires patch occupancy, colonization, and extinction dynamics before and after the invasion. Such data are simply unavailable for nearly all invaded systems. We argue, however, that the absence of such information should not

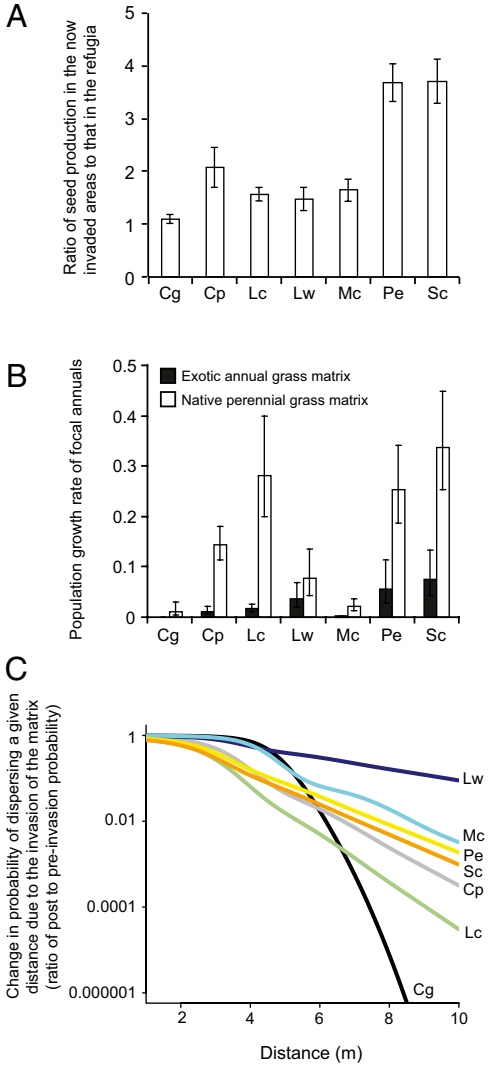

Fig. 2. Impact of invasion on local population sizes and dispersal. (*A*) When competing only against other native annual species, the focal annuals have significantly higher finite rates of increase in the area now occupied by invasive grasses than in their current refugia. Bars show mean ratio ± SE, with ratios greater than 1 indicating that areas now dominated by invasive species are optimal for the native plants. (*B*) Native annuals had higher finite rates of increase among native bunchgrasses than among invasive grasses (mean R ± SE) in the matrix habitat. Data are not presented as ratios because the finite rate of increase of *Chaenactis* among exotic grasses was zero. (*C*) Lower finite rates of increase of native annuals in invaded habitat greatly reduce connectivity by decreasing multigenerational dispersal through the matrix. Curves show the effect on the probability of dispersal of lowering species' finite rates of increase in the matrix after invasion, given a mean dispersal distance of $\sigma = 1$. The effect of dispersal through the matrix is calculated assuming that offspring from a parent plant could not persist for more than 30 y in the matrix (i.e., $n_{max} = 30$ in Eq. **S5**). Cg, *Chaenactis galibriuscula*; Cp, *Chorizanthe palmerii*; Lc, *Lasthenia californica*; Lw, *Lotus wrangelianus*; Mc, *Micropus californicus*; Pe, *Plantago erecta*; Sc, *Salvia columberiae*.

prevent ecologists from exploring extinction debts in invaded landscapes, even if considerable uncertainty surrounds such efforts. To show how this might be accomplished, we field-parameterize the model for seven experimentally tractable focal annual plants (Table S3). We then predict the influence of invasion on their metapopulation persistence and explore the sensitivity of these results to variation in model parameters, such as loss of habitat to invasion and dispersal ability.

Some model parameters were assumed to be unaffected by invasion, including the spatial location of the centroid of suitable habitats, seed production per unit area in current refugia habitat (μ), and species' dispersal distances (σ). Seed production per unit area, μ, was measured in plots sown with the focal species evenly spaced along transects through the refugia. Seed dispersal rates, σ, were parameterized with empirical relationships between dispersal distances, plant height, and dispersal syndrome from the literature (21), and were then validated with field data. According to published relationships, mean dispersal distances for our species range from 0.1 to 0.5 m, with the lower estimate for the shortest plant with no obvious dispersal mechanism and the higher estimate for the tallest of the wind-dispersed plants. Seeds trapped at various distances from parental populations at our field site confirmed these extremely low mean dispersal distances (*SI Materials and Methods* and Table S4). To predict invader effects on metapopulation persistence conservatively, we assumed a mean dispersal distance of 0.8 m ($\sigma = 1$) for all species but also explore more restricted dispersal (mean distance = 0.4 m, $\sigma = 0.5$; *SI Materials and Methods*).

The parameters affected by invasion were (*i*) the relative quality of the habitat from which the native species were displaced (which determines w'), (*ii*) native per capita population growth rates in the matrix area between habitat patches (R'), and (*iii*) the area of each patch from which native species were displaced ($A * H_F$). To parameterize *i*, the relative quality of the habitat lost, we grew a community of the native annual plants in a refugia habitat and in a habitat adjacent to the refugia in plots where we experimentally removed exotic grasses.

Estimating how invasion altered native annual growth rates in the matrix and the size of each patch is more complicated. Although the details of the preinvasion landscape are uncertain, native bunchgrasses very likely dominated the matrix habitat between outcrops before exotic grass invasion. This common assumption for California grasslands (9, 24) is supported by the frequent occurrence of the native bunchgrass *Stipa pulchra* in the matrix habitat even today (19, 23). Thus, to estimate native annual growth rates in the matrix (R and R'), we measured the population growth rates of focal native annuals sown into matrix plots dominated by either European annual grasses or native perennials. Bunchgrass dominance of the matrix would mean that native forbs suffered the negative effects of a fragmented landscape even before invasion. Given that the native forbs themselves may have once dominated the matrix, our assumption conservatively predicts the impact of invasion.

In addition to changing the nature of the matrix, exotic grass invasion likely reduced the size of the rocky hummocks by invading their margins (9, 24); however, if it did so, the extent is unknown. We therefore explored a range of invasion scenarios. At one extreme, invasive grasses only displaced native bunchgrasses in the matrix between refugia, and therefore did not have an impact on refugia area ($H_F = 1$). At the other extreme, we assume that in addition to replacing the native bunchgrass matrix, European annual grasses encroached into the rocky hummocks from the margins, reducing their area by up to 50% (Fig. 1*B*, dashed vs. solid lines; $H_F = 0.5$). This second extreme means that less than 10% of the area currently occupied by nonnative plants would have formerly been native annual habitat.

Results and Discussion

We found that finite rates of increase of native annual species were up to 3.5-fold greater in habitat now dominated by European grasses than in their current habitat (generalized least squares, $P < 0.05$; Fig. 2*A* and Table S1). This indicates that not only does European grass encroachment of the patches, to the extent that it occurs, remove habitat suitable to the focal native annual plant species but it removes what is otherwise superior habitat.

Even if preinvasion patches were double in size, a large grass matrix remains (Fig. 1*B*). However, the ability of the focal annual plants to disperse through the matrix, and thereby colonize other patches, was greater before invasion. We found that all native annual plants had finite rates of increase less than 1 in matrix plots dominated by native perennial bunchgrasses, the presumed

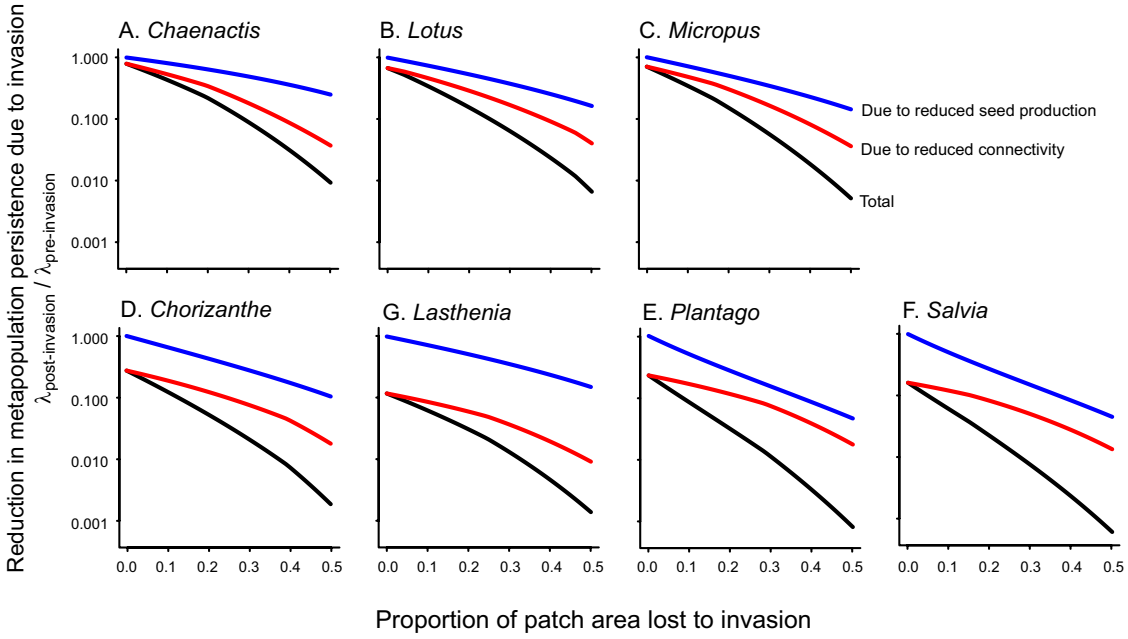

Fig. 3. Impact of loss of seed production (blue line) and reduction in habitat connectivity (red line) on metapopulation viability (black line; joint contribution) for the seven focal species. Seed production alters both colonization and extinction dynamics, whereas loss in connectivity results from a reduction in habitat size and alteration of dispersal through the matrix. Panels correspond to the species listed by genus (full names are given in Fig. 2).

former dominant (Fig. 2*B*). Thus, before European grass invasion, much of the matrix between patches was too competitive for the persistence of the focal species. However, finite rates of increase (R) were significantly higher among native bunchgrasses than invasive grasses (mean: $R = 0.16$ and $R = 0.03$, respectively; Fig. 2*B* and Table S2). Because the dispersal permeability of the matrix depends on these growth rates (Eq. **2** and Eq. **S5**), parameterizing Eq. **2** with R values preinvasion and postinvasion suggests that European grass invasion of the matrix alone imposes an order of magnitude reduction in the probability of colonizing a patch only several meters away (Fig. 2*C* and Fig. S3).

We can partition invader effects on metapopulation persistence ($\lambda_{post-inv}/\ \lambda_{pre-inv}$) into the multiplicative effects of reduced seed production (affecting both colonization and stochastic extinction) and reduced connectivity (Eqs. **4** and **5**, Fig. 3, and Eq. **S6*B***). We found that for all species and degrees of area loss, the reduction in metapopulation persistence due to reduced connectivity (red line in Fig. 3) was greater than the reduction due to lost seed production (blue line in Fig. 3, which lies above the red line in all panels of Fig. 3). Of note, the y intercept of the red line (zero patch area lost) shows the effect of reduced landscape permeability caused by the replacement of the native bunchgrass matrix with European grasses in the absence of any change in patch size, one of the invasion scenarios for this system. This effect reduces metapopulation persistence by up to an order of magnitude, and it was variable across species (Fig. 3 and Fig. S4). It was strongest for species like *Lasthenia*, which grew much better in the matrix with native perennial bunchgrasses than with European annuals. The negative slope to the connectivity line reflects the effect of increasing isolation of patches as their area is lost. Holding connectivity constant, the metapopulation persistence of all species declined with the reduced seed production associated with habitat area loss (blue line in Fig. 3). This effect was most severe for species like *Plantago* and *Salvia* (Fig. 3 *E* and *F*) that grew relatively well in the lost habitat area (Fig. 2*A*).

We can also explore the long-term impact of invasion under the scenario in which European grasses replace the native bunchgrasses in the matrix and also reduce the size of the native annual patches to varying degrees. Assuming a 50% loss of habitat due to European grass invasion, these collective invader impacts reduced metapopulation persistence ($\lambda_{post-inv}/\ \lambda_{pre-inv}$; Eqs. **4** and **5** and Eq. **S6*B***) by two to more than three orders of magnitude for the seven focal annual plants (black lines in Fig. 3 and Fig. S4). Although their preinvasion patch occupancy is unknown, all would persist if they occupied more than 45% of patches before invasion and none would persist having occupied only 10% of patches (Fig. 4*A* using Eq. **5**). If we assumed that grass invasion reduced patch area by only 20%, we still predict a roughly one order of magnitude decline in metapopulation persistence; all populations with more than 18% preinvasion occupancy would persist (Fig. 4*A*). Given that most metacommunities consist of species that occur in a low proportion of potential sites (26–28), the local extinction of many native plant species is likely when invader impacts are as great as seen in this ecosystem.

Next, we show that for species that cannot persist with invasion, their time to extinction can still be on the order of hundreds of years in this landscape. Because the model used does not predict times to extinction, we used simulations to generate extinction time lines for an "average" species following invasion (*SI Materials and Methods*, *Model Simulations and Numerical Solutions*). This average species possesses the average of all demographic rates from the seven common taxa but not their local density, which we varied in our simulations (Table S5). Consistent with earlier results, we found that only some combinations of patch area loss and local density led to extinction (Fig. 4*B*). When the species fell below the extinction threshold (Eq. **1**), extinction happened rapidly if the species was sparse and the habitat loss too great. However, for a wide range of habitat area loss and population densities, times to extinction were long, upward of several hundred years (Fig. 4*B*). Long extinction times after habitat destruction are characteristic of

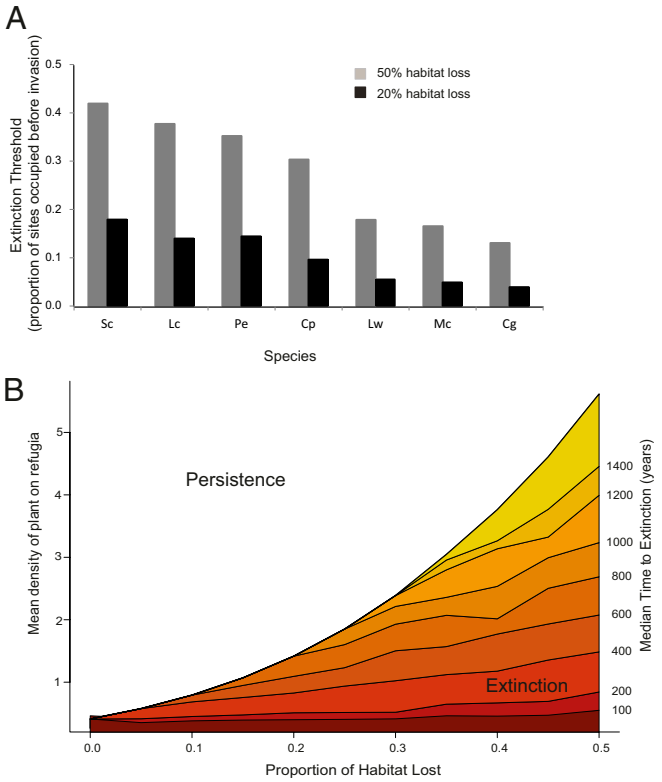

Fig. 4. Extinction thresholds and times to extinction for species in an extinction debt. (*A*) Extinction threshold is the minimum proportion of habitat that a species must occupy before invasion to avoid falling into an extinction debt following invasion. Estimates are based on incorporating both species-specific responses to invaders (black lines in Fig. 3) and the level of habitat loss shown into Eq. **5**. Species abbreviations are given in Fig. 2. (*B*) Median time to extinction for an average species with a given mean density and proportion of habitat lost to invaders. Estimates are based on simulations for an "average" species containing the mean trait values of the seven focal species.

many metapopulations (18) and were also found with very different values of c and e, two model parameters that we can only approximate (*SI Materials and Methods*).

Finally, we discuss the sensitivity of our metapopulation persistence predictions to the uncertainty that naturally arises with many of the parameters. The estimated dispersal distances were short, which can greatly affect the impact of connectivity (compare Figs. 2*C* and 3 with Figs. S3 and S4). We therefore calculated patch connectivity with upper bound dispersal distances that conservatively estimate the impact of changes in connectivity (Figs. 2*C* and 3) and with estimated mean dispersal distances (Figs. S3 and S4). Increasing the mean dispersal distance significantly increases metapopulation viability, more so than changing the dispersal kernel to one with a "fatter tail" (*SI Materials and Methods*, *Model assumptions*). Similarly, uncertainty in the fraction of the patch area lost motivated us to explore the effects of a range of plausible losses of patch area, and results differ as shown in Figs. 3 and 4. Our inclusion of seven focal species, all with their own vital rates (Fig. 2 *A* and *B* and Tables S1 and S2), also gives an indication of how results vary across parameter combinations found for species in the system. Finally, the sensitivity of extinction debt time lines to parameters c and e was explored. In several cases, the sensitivity analyses indicate consistent predictions across a range of parameter values (e.g., Fig. S5). We found, for example, a greater effect of reduced connectivity vs. reduced seed production on metapopulation persistence in invaded landscapes for all focal species, regardless of the mean dispersal distance incorporated (Fig. 3). Other results were more sensitive to parameter values, as suggested by the variation among species in their overall sensitivity to invader impacts (Fig. 3 and Fig.

S4). A final source of uncertainty arises from the fact that our study examines only a subset of the processes that negatively affect native metapopulations following invasion. Other factors, such as large-scale environmental stochasticity, demographic stochasticity at the scale of the entire metapopulation, and changes to pollinator dynamics following greater fragmentation, should all exacerbate the effects that we report (29).

We conclude that plant invasions relegating native populations to isolated patches can greatly reduce their metapopulation viability. Even under low levels of invasion, most species in our system that occupy less than 10% of patches may enter an extinction debt (Fig. 4*A*). In studies of metapopulations around the world, plant species most commonly fall into this low-occupancy range (28). Moreover, these extinction debts may take hundreds of years to play out. In a world with a rapidly changing climate, it is tempting to regard invader impacts that occur with 100-y time lags as a lower priority concern. However, invasions that reduce metapopulation viability by limiting connectivity or local population size may exacerbate the effects of climate change because these factors also limit opportunities for migration (30) and evolution (31), which are key processes for persistence in a changing world. Recent suggestions that plant invasions fail to drive native plant extinctions may be premature.

Materials and Methods

We conducted experiments in an 8-ha area at the northern edge of the Sedgwick Reserve (34° 44′ 20″ North, 120° 01′ 34″ West). The area has a natural metapopulation structure, with refugia of native annual plants occurring on slightly raised mounds with coarse soils (9, 19). We selected seven native annual species that were abundant enough to provide sufficient seed for our experiments (species are listed in Fig. 2 and *SI Materials and Methods*). The area between refugia is almost completely covered with exotic grasses, mainly *Avena fatua*, *Avena barbata*, and *Bromus* sp. Pockets of native bunchgrasses (mainly *S. pulchra*) persist in small patches among invasive grasses. Initial categorization of the landscape was performed using images from Google Earth, according to the method of Gram et al. (19). We subsequently performed detailed mapping of a portion of the site using a global positioning system and ground measurements, and we used geographic information system (GIS) tools (ArcGIS) to calculate patch areas and centroids; the resulting detailed map (Fig. 1*B*) was used for all analyses.

Habitat Quality Experiment. We evaluated the relative seed production in current refugia vs. invaded habitat by sowing 3 $g \cdot m^{-2}$ of native seed per species into 20 × 20-cm plots cleared of competitors on refugia and also immediately adjacent to refugia in invaded habitat. In total, we had 96 plots (48 in each habitat type) distributed across 12 of the larger refugia in the study area. We used half of the plots in each habitat type to estimate germination rates and the other half to estimate per capita seed production. Finite rates of increase were calculated for each sown species by summing its seed production and the carryover of ungerminated seeds in the seed bank (*SI Materials and Methods*) and dividing through by the seeds added. Seed bank carryover was the product of the number of added seeds, one minus the germination rate, and the seed survival fraction (estimated by measuring seed viability before and after a year of burial in mesh bags). Mean seed density on refugia (μ) was estimated for each species from the sum of seed production and seed bank carryover in refugia plots.

Matrix Permeability Experiment. Matrix permeability (R) was estimated by sowing 3 $g \cdot m^{-2}$ of seed per species into 10 sets of paired plots that were placed less than 1.5 m from each other. Two plots were placed in each type of grass (native perennial or exotic annual) at each location: high-density plots, sown with seed densities from natural refugia, and low-density plots in which only small numbers of native annual seed were added. Because the two densities gave similar results, they were combined for analysis. We estimated R as the seed production in each plot divided by the number of seeds added. Results from matrix permeability and habitat quality experiments were first tested with nested distance-based permutation multivariate ANOVA and, following significant results, with separate generalized linear mixed models for each species.

Seed dispersal rates were first estimated from well-established relationships between dispersal distance, plant height, and dispersal syndrome (21). We used two empirical methods to test the validity of these estimates. We created "false refugia" by clearing circular 50-m^2 areas of invasive grasses, with edges ranging from 0.5 to 7 m from the nearest refugia. Germinants of our focal species were counted the year after these refugia were created. In addition, we chose two refugia that contained all species and placed seed traps (28 × 52 cm, 92 seed traps total) at distances up to 8 m from the refugia edge.

ACKNOWLEDGMENTS. We thank Florian Altermatt, Susan Harrison, Andrew MacDougall, and Helen Rodd for suggestions. Research was supported by the Packard Foundation (J.M.L.) and the Natural Sciences and Engineering Research Council of Canada (B.G.).

1. Sax DF, Gaines SD (2008) Colloquium paper: Species invasions and extinction: The future of native biodiversity on islands. *Proc Natl Acad Sci USA* 105(Suppl 1):11490–11497.
2. Wilcove DS, Rothstein D, Dubow J, Phillips A, Losos E (1998) Quantifying threats to imperiled species in the United States. *Bioscience* 48(8):607–615.
3. Gurevitch J, Padilla DK (2004) Are invasive species a major cause of extinctions? *Trends Ecol Evol* 19(9):470–474.
4. Sax DF, Gaines SD, Brown JH (2002) Species invasions exceed extinctions on islands worldwide: A comparative study of plants and birds. *Am Nat* 160(6):766–783.
5. Sax DF, et al. (2007) Ecological and evolutionary insights from species invasions. *Trends Ecol Evol* 22(9):465–471.
6. Davis MA, et al. (2011) Don't judge species on their origins. *Nature* 474(7350):153–154.
7. Hobbs RJ, Mooney HA (1998) Broadening the extinction debate: Population deletions and additions in California and Western Australia. *Conserv Biol* 12(2):271–283.
8. Huenneke LF, Hamburg SP, Koide R, Mooney HA, Vitousek PM (1990) Effects of soil resources on plant invasion and community structure in Californian serpentine grassland. *Ecology* 71(2):478–491.
9. Seabloom EW, et al. (2003) Competition, seed limitation, disturbance, and reestablishment of California native annual forbs. *Ecol Appl* 13(3):575–592.
10. Daehler CC (2003) Performance comparisons of co-occurring native and alien invasive plants: Implications for conservation and restoration. *Annu Rev Ecol Evol Syst* 34:183–211.
11. MacDougall AS, Turkington R (2006) Dispersal, competition, and shifting patterns of diversity in a degraded oak savanna. *Ecology* 87(7):1831–1843.
12. Hanski I (1994) Patch-occupancy dynamics in fragmented landscapes. *Trends Ecol Evol* 9(4):131–135.
13. Hanski I, Ovaskainen O (2000) The metapopulation capacity of a fragmented landscape. *Nature* 404(6779):755–758.
14. Ovaskainen O, Hanski I (2001) Spatially structured metapopulation models: Global and local assessment of metapopulation capacity. *Theor Popul Biol* 60(4):281–302.
15. Vellend M, et al. (2006) Extinction debt of forest plants persists for more than a century following habitat fragmentation. *Ecology* 87(3):542–548.
16. Kuussaari M, et al. (2009) Extinction debt: A challenge for biodiversity conservation. *Trends Ecol Evol* 24(10):564–571.
17. Malanson GP (2008) Extinction debt: Origins, developments, and applications of a biogeographical trope. *Prog Phys Geogr* 32:277–291.
18. Tilman D, May RM, Lehman CL, Nowak MA (1994) Habitat destruction and the extinction debt. *Nature* 371:65–66.
19. Gram WK, et al. (2004) Distribution of plants in a California serpentine grassland: Are rocky hummocks spatial refuges for native species? *Plant Ecol* 172(2):159–171.
20. Safford H, Viers J, Harrison S (2005) Serpentine endemism in the California flora: A database of serpentine affinity. *Madrono* 52(4):222–257.
21. Thomson FJ, Moles AT, Auld TD, Kingsford RT (2011) Seed dispersal distance is more strongly correlated with plant height than with seed mass. *J Ecol* 99(6):1299–1307.
22. Hanski I (1994) A practical model of metapopulation dynamics. *J Anim Ecol* 63(1):151–162.
23. Seabloom EW, Harpole WS, Reichman OJ, Tilman D (2003) Invasion, competitive dominance, and resource use by exotic and native California grassland species. *Proc Natl Acad Sci USA* 100(23):13384–13389.
24. Keeley JE (1990) *Endangered Plant Communities of Southern California*, ed Schoenherr AA (Southern California Botanists, Fullerton, CA), pp 2–23.
25. Wolf A (2001) Conservation of endemic plants in serpentine landscapes. *Biol Conserv* 100(1):35–44.
26. Harrison S, Maron J, Huxel G (2000) Regional turnover and fluctuation in populations of five pants confined to serpentine seeps. *Conserv Biol* 14(3):769–779.
27. Hanski I (1982) Dynamics of regional distribution: The core and satellite species hypothesis. *Oikos* 38(2):210–221.
28. Scheiner SM, Rey-Benayas JM (1997) Placing empirical limits on metapopulation models for terrestrial plants. *Evol Ecol* 11(3):275–288.
29. Gaggiotti O, Hanski I (2004) *Ecology, Genetics, and Evolution of Metapopulations*, eds Hanski I, Gaggiotti O (Academic, San Diego), pp 337–366.
30. Pachepsky E, Levine JM (2011) Density dependence slows invader spread in fragmented landscapes. *Am Nat* 177(1):18–28.
31. Bell G, Gonzalez A (2011) Adaptation and evolutionary rescue in metapopulations experiencing environmental deterioration. *Science* 332(6035):1327–1330.

Supporting Information

Gilbert and Levine 10.1073/pnas.1212375110

SI Materials and Methods

Model Structure. Our study builds on a spatially explicit, discrete time patch occupancy model (Eq. **1**). The model structure assumes that local population dynamics are fast relative to colonization dynamics, as seems reasonable for the focal ecosystem. It also assumes that metapopulation extinction only occurs when it is the deterministic outcome of the colonization and extinction dynamics. It does not predict stochastic global extinctions, as might be likely when metapopulation sizes are small.

Here, we provide a more detailed description of the metapopulation model. The model assumes that the change in the probability of occurrence (p) of a focal species in a patch is the difference between the colonization probability (C) and extinction probability (E). As given in Eq. **1**, the probability of colonization for patch i is:

$$C_i(p) = \frac{S_i(p)}{S_i(p) + \frac{1}{c}}, \text{ where } S_i(p) = \sum_{j \neq i} \mu A_j p_j K_{ij}, \qquad \textbf{[S1}\boldsymbol{A}\textbf{]}$$

and the probability of extinction is:

$$E_i(p) = eD_i(1 - C_i(p)), \text{ where } D_i = (1/\mu A_i). \qquad \textbf{[S1}\boldsymbol{B}\textbf{]}$$

The patch area is denoted A, and μ represents the seed production of the focal species per unit area of patch. In annual plants, seed production is a measure of both local population size and the number of potential dispersers. The colonization probability (Eq. **S1*A***) is a saturating function of the distance-weighted seed production in all other patches (S) and has a value of 0.5 when the number of seeds (S) equals $1/c$. The dispersal probability between patches (K_{ij}) is developed further below. Extinction is inversely related to the population size in the focal patch Eq. **S1*B***). The species-specific parameter e gives the probability that a small patch (supporting one individual, on average) would go locally extinct in the absence of a rescue effect. This rescue effect, $[1 - C_i(p)]$, reduces the chance of extinction.

The function $g_i(p)$, where

$$g_i(p) = C_i(p)/E_i(p), \qquad \textbf{[S2]}$$

describes the expected frequency of colonization events relative to extinction events for each patch i. Building on the methods developed by Ovaskainen and Hanski (1), our model is what they characterize as a Levins-type model, with $g_i(p) = cS_i(p)/eD_i$. For these types of models, when evaluated at $P = 0$, the leading eigenvalue (λ) of the Jacobian matrix of the function g [the mathematical matrix **M** with elements $\partial g_i(p)/\partial p_j$] defines the invasion capacity of the metapopulation (i.e., whether the metapopulation can grow from an initial low occupancy). The leading eigenvalue also defines the metapopulation capacity, the nonzero equilibrium for the metapopulation; it provides a very close approximation of the spatially weighted equilibrium site occupancy for the spatially realistic Levins model ($p^* \approx 1 - 1/\lambda$) (1, 2). We use this relationship to arrive at Eq. **5**.

Standard estimation techniques for determining metapopulation parameters assume that the metapopulation under study is in a quasiequilibrium state, meaning that the incidence (site occupancy) of a species reflects its colonization and extinction rates (3). However, when an extinction debt is present, the metapopulation does not have a nonzero quasiequilibrium by definition. As a result, site occupancy cannot be used to infer colonization and extinction rates. Instead, the individual parameters of the model (Eq. **4**) must be estimated experimentally. Our approach of evaluating the ratio of eigenvalues (Eq. **5**) allows us to eliminate several parameters that do not change following invasion, thus minimizing the number of parameters that need to be estimated (Eq. **S6*B***).

Dispersal function. The seed arrival function (S_i in Eqs. **1*B*** and **3** and Eq. **S1*A***) describes the number of seeds that are expected to arrive at site i. Based on the focal California system, we assume passive, isometric dispersal. The size and distance of the "target patch" affect the number of arriving seeds as follows. The probability that each seed dispersing from patch j arrives in patch i is first determined by the probability $[p(x)]$ of dispersing the distance interval $d_{ij} \pm radius_i$ (Fig. S1). This defines a ring around the source patch, and the fraction of that ring that is occupied by the target patch i, d_{ij} distance away, is equal to $\sqrt{A_i}/(4d_{ij}\sqrt{\pi})$. With a normal dispersal kernel, this geometric framework gives:

$$S_i = \mu k \sum_{j \neq i} A_j \frac{\sqrt{A_i}}{\sigma d_{ij}} \int_{d_{ij-radius_i}}^{d_{ij+radius_i}} \exp\left(-x^2/2\sigma^2\right). \qquad \textbf{[S3]}$$

The constant k, which is equal to $2^{-3/2}\pi^{-1}$, normalizes the dispersal kernel and the target area approximation such that the total probability of dispersal to all possible locations is equal to 1.

We checked this approximation with simulations in which large numbers of seeds produced in a source patch dispersed following a normal dispersal kernel and the probability of arriving at other patches of varying size (radius) and at various distances away from the source patch was measured. These simulations showed that the approximation (Eq. **S3**) accurately describes the effect of target size and distance on seed arrival ($R^2 = 0.998$) when the minimum distance between the closest edges of two patches is greater than the rms dispersal distance (σ) and underestimates the probability of seed arrival when this distance is smaller than σ. With this rule, the proportion of pairwise site distances in our study system that are underestimated is 0.001.

Eq. **S3** was then used to estimate the impact of reducing patch size on the dispersal between patches, including the fact that patches become effectively further apart. It should be noted that this "target area" effect is appropriate when invasive species have caused patch areas to shrink by encroaching on the edges of pre-invasion habitat area. In areas where patches have been invaded such that the area remains constant but native densities decline, only the per area seed production (μ, Table S1) term changes.

Eq. **S3** assumes that dispersal cannot proceed by spreading through the matrix over successive generations. To include this process, we first rewrite the equation such that it expresses the probability that a single seed disperses to the target patch:

$$P(\text{one seed arriving}) = k \frac{\sqrt{A_i}}{\sigma d_{ij}} \int \exp\left(-x^2/2\sigma^2\right), \qquad \textbf{[S4}\boldsymbol{A}\textbf{]}$$

where the integral is again defined by the interval $d_{ij} \pm radius_i$. Given that plants in our system can produce seeds in the matrix (but still have finite rates of increase less than 1), we developed a prediction for dispersal when a seed landing in the matrix could potentially produce other seeds. In particular, we modeled dispersal through the matrix as a random walk that allows the focal

seed or its offspring to disperse from habitat patch j to i. Each step in the walk, apart from the initial dispersal from patch j, is taken with probability R (the finite rate of increase or average number of offspring per seed in the matrix). The probability of a seed (or its offspring) dispersing from patch j to patch i in n generations is defined by its kernel, Q_n. The probability of the seed dispersing in the first generation (i.e., directly) is given in Eq. **S4*A***. The probability of it arriving in the second generation is given by:

$$Q_2 = Rk\frac{\sqrt{A_i}}{\sqrt{2}\sigma d_{ij}}\int\left(\exp\left(-x^2/2\left(\sqrt{2}\sigma\right)^2\right)\right)dx(1-Q_1). \qquad \textbf{[S4B]}$$

The final term in Eq. **S4*B*** $(1-Q_1)$ accounts for the fact that a seed cannot colonize a patch twice (i.e., the probability can never sum to more than 1). The $\sqrt{2}$ that scales the rms dispersal distance (σ) is a result of the random walk. The variance of a random walk is equal to $n\sigma^2$, where n is the number of steps taken and σ^2 is the variance of the normal dispersal kernel. The integral remains unchanged from Eq. **S4*A*** because it measures the distance between patches. Following this random walk over several generations gives:

$$Q_3 = R^2k\frac{\sqrt{A_i}}{\sqrt{3}\sigma d_{ij}}\int\left(\exp\left(-x^2/2\left(\sqrt{3}\sigma\right)^2\right)\right)dx(1-Q_2)\ldots$$

$$Q_n = R^{n-1}k\frac{1}{\sqrt{n}}\frac{\sqrt{A_i}}{\sigma d_{ij}}\int\left(\exp\left(-x^2/2\left(\sqrt{n}\sigma\right)^2\right)\right)dx(1-Q_{n-1}). \qquad \textbf{[S4C]}$$

The total probability of a seed, or its offspring, reaching patch i [i.e., K_{ij}] is the sum of these probabilities:

$$K_{ij} = \sum_{n=1}^{\infty} Q_n. \qquad \textbf{[S5]}$$

The formulations given in Eqs. **S4** and **S5** are based on a model in which a seed and its offspring can only disperse between two patches. They also assume that the surviving progeny of any seed is only considered to disperse if the seed did not reach patch j (the $1-Q_{n-1}$ term in the final brackets in Eq. **S4**); this term eliminates multiple colonization events. In reality, and for areas with multiple "recipient" patches, this correction factor for multiple colonization events should include the probability of the seed establishing on any other patch, because a seed can only colonize a single patch (i.e., $1 - \sum Q_{n-1}$, with the summation calculated over all sites). However, simulations indicate that this probability is low enough for sparsely distributed habitats (habitats occupying <12% of the region; our study site is ~5% of the region) that it has little effect on the probability of dispersal.

We checked the approximation of our dispersal model, including multigenerational spread through the matrix with simulations. As before, we assembled hypothetical landscapes with patches varying in distance from the source patch but now including multigenerational dispersal through the matrix with $0 < R < 1$. These simulations indicate that Eq. **S5** provides a good fit to dispersal probabilities even for landscapes with multiple patches, as long as those patches are sparsely distributed (all R^2 values >0.996).

Although Eq. **S5** should be calculated over an infinite number of generations, the low survival rates in the matrix between rocky outcrops (the R^{n-1} term) quickly reduces the probability of colonization to near zero after about 10 generations. For example, numerical analysis shows that even for relatively large sink populations with $R = 0.33$ (i.e., one in three seeds, on average, produces a viable seed), $R^{n-1} \approx 10^{-7}$ in 15 generations. The largest estimate of R in our study was for *Salvia* ($R = 0.34$), and the lowest was for *Chaenactis* ($R = 0.01$; Table S2).

We evaluate the effects of invasion on dispersal probabilities by multiplying the finite rate of increase rate in the matrix (R) by R', the finite rate of increase rate in the invaded matrix relative to that in the native bunchgrass (Eq. **S6**). All species but one had nonzero finite rates of increase when grown among exotic grasses; for these species, R' estimates ranged from one-half to 1/17 (Table S2). Invasion also modifies the area of patches, which reduces both A_i and the range of the integral evaluated in Eqs. **S3**–**S5**. These latter effects are shown in Fig. 3.

Incorporating invasion into the model. When we incorporate the effects of invasion on seed production, habitat area, and matrix permeability into our model, the elements of the metapopulation matrix become:

$$m_{ij} = \frac{ck\mu^2 A_i^{1.5}A_j}{e\sigma d_{ij}}\left(w'H_F\right)^2 \sqrt{H_F}\sum_{n=1}^{\infty}\left[\frac{1}{\sqrt{n}}\left[R\left(R'\right)\right]^{n-1}\int\left(\exp\left(-d_{ij}^2/2n\sigma^2\right)\right)dx(1-Q_{n-1})\right], \qquad \textbf{[S6A]}$$

and

$$m_{ij_{post-inv}}/m_{ij_{post-inv}} = \left(w'H_F\right)^2\sqrt{H_F}\,\frac{\sum_{n=1}^{\infty}\left[\frac{1}{\sqrt{n}}\left[R\left(R'\right)\right]^{n-1}\int\left(\exp\left(-d_{ij}^2/2n\sigma^2\right)\right)dx(1-Q_{n-1})\right]}{\sum_{n=1}^{\infty}\left[\frac{1}{\sqrt{n}}R^{n-1}\int\left(\exp\left(-d_{ij}^2/2n\sigma^2\right)\right)dx(1-Q_{n-1})\right]}, \qquad \textbf{[S6B]}$$

with w' defined as the ratio of seed density postinvasion to preinvasion. It depends on both the seed production in habitat lost to invaders and the fraction of habitat remaining (H_F). In particular, if υ is the ratio of seed production in habitat lost to invaders to seed production in refugia (Fig. 2 and Table S1), $w' = \frac{1}{H_F(1-\upsilon)+\upsilon}$. The effects of seed loss and reduced connectivity can be separated using Eq. **S6*B***, with the effect of lost seed production (on colonization and extinction) given by the term $(w'H_F)^2$ and the remainder of the equation giving the loss in connectivity due to reduced target area (patch size) and reduced matrix permeability. Changes to seed production act as a scalar, such that $\lambda_{\text{postinvasion}} = \lambda_{\text{preinvasion}}\,(w'H_F)^2$ in the absence of a change in connectivity. Unlike seed production, connectivity depends on the geographic positions of refugia relative to each other, and changes in connectivity therefore do not scale λ in a uniform manner. The complete list of parameters included in our model and how they are parameterized is given in Table S3.

Model assumptions. To estimate the effects of invasion in this landscape, three important assumptions about the population dynamics of the species were needed. The first assumption is that extinction probability in a patch scales inversely with local pop-

ulation size (Eq. **1*C*** and Eq. **S1*B***). This assumption follows Hanski's model of local extinction (3, 4), where extinction $\propto 1/A^x$. A small value of x corresponds to a high level of environmental stochasticity; in our study system, species' finite rates of increase had coefficients of variation that ranged from 0.36 to 1 when measured over 3 y (5), indicating a high level of variability consistent with $x \approx 1$, as was used in our model. Increasing the value of x increases the sensitivity of the metapopulation to habitat loss, and our estimates here are therefore conservative in terms of the impacts of habitat loss.

The second assumption is related to the consistency of population growth rates over time. Although the model allows for fluctuating population growth rates through time, we assume that the (geometric) mean population growth rate on refugia has not changed from that before invasion. Similarly, we assume that the mean ratio of population growth rates on refugia to those in the invaded portion of habitat patches stays constant over time.

The third assumption is in the dispersal approximation, which assumes that seed dispersal is represented well by a normal dispersal kernel (Eq. **S4**). This shape of kernel can be derived from first principles and is appropriate for many plant species (6). However, a "fat-tailed" distribution may be more appropriate for some species. The random walk that we used to model matrix permeability (Eq. **S4**) tends to a normal distribution of dispersal distances over many generations, even when a different kernel describes seed dispersal in a single generation (6). The normal distribution is numerically tractable for this reason, whereas other kernels are not. Although we are not able to find a numerical solution for fat-tailed distributions, a sensitivity analysis with the exponential dispersal kernel (a fatter tailed kernel) indicates that the results of Eq. **S4** are more sensitive to mean dispersal distance than to the shape of the kernel, especially for refugia that are relatively close together (and therefore contribute more strongly to λ). Similarly, a sensitivity analysis showed that a change in the mean dispersal distance of a normal kernel (as used here) causes a larger change in metapopulation viability (λ) than changing the shape of the dispersal kernel [sensitivity tested using fatter tailed distributions – the exponential distribution and the t-distribution with 3 df (7), all scaled to an equal mean dispersal distance]. Because of this greater sensitivity to mean dispersal distance, our use of a high dispersal distance ($\sigma = 1$) likely underestimates the impacts of changing connectivity on metapopulation persistence. To provide a range of realistic predictions, we also consider a dispersal distance within the expected range of the focal species ($\sigma = 0.5$; Figs. S2 and S3).

Model Simulations and Numerical Solutions. We used numerical solutions of the model to determine the loss of metapopulation viability following invasion and how this loss is partitioned between connectivity effects and seed production effects (Fig. 3, Fig. S4, and Eq. **S6*B***). Our estimates of extinction thresholds for each species (Eq. **5** and Fig. 4*A*) and the effects of invasion on dispersal rates (Eqs. **S4** and **S5** and Fig. 2*C*) are also based on numerical solutions.

Simulation modeling was used for two purposes. First, as described in the section on the dispersal model, we used simulations to test our analytical approximations of the dispersal function (e.g., Eqs. **S3**–**S5**). Second, we used simulations to generate time lines to extinction (Fig. 4*B* and Fig. S5). Although our model does predict the conditions under which extinction debts will occur (Eq. **5**), simulations are needed to give expected time lines for extinction. For all such simulations, we used the metapopulation modeling approach outlined by Hanski (8), in which all refugia are modeled as distinct, circular patches surrounded by matrix habitat. This approach is different from one in which the matrix is divided into a lattice of patches of suboptimal quality; our dispersal kernel (Eqs. **S4** and **S5**) accounts for the matrix habitat without requiring this step. The extinction time line simulations were run as follows.

We created a grid of plant densities (values of μ) by habitat loss scenarios. In total, we used 22 values of μ and 11 habitat loss values (H_F ranging from 1 to 0.5) for 242 scenarios. For all parameters (Table S3), we used the average value from all species in our experiment (Table S5 and additional parameters for simulation, as explained below), except for average seeds per unit area (μ). Given all the parameters (except μ), we first solved Eq. **S6*B*** for the ratio of λ preinvasion vs. postinvasion. This ratio can then be used in Eq. **5** to determine the critical p^* value at which an extinction debt would emerge. Because the leading eigenvalue of the mathematical matrix **M** has a known relationship with μ ($\lambda \propto \mu^2$; seen from the scalar μ^2 in **M** in Eq. **S6*A***), we were then able to select a range of values for μ to generate a range of p^* values below this critical value.

For each value of μ and H_F, we solved the metapopulation model for the expected occupancies of each patch before invasion. In particular, in accordance with the study by Ovaskainen and Hanski (1) (equations **3** and **4** in ref. 1), we define $h(p)$ as a function such that $h_i(p) = g_i(p)/(\mathbf{1} + g_i(p))$. We then iteratively solved for p using the equation $p_{t+1} = h(p_t)$ employing an initial value for p (p_0) that was uniformly low in all patches. The solution to the iteration gave the expected occupancy of each patch before invasion [full details are provided in the study by Ovaskainen and Hanski (1)].

We then created 150 "preinvasion landscapes" for each combination of habitat loss and plant density. These landscapes were spatially identical to the current postinvasion landscape (Fig. 1*B*), except that the area of each patch i was equal to its preinvasion size, A_i/H_F. In each of these 150 landscapes, the initial occupancy of each patch was random (determined by a Bernoulli trial) with a probability equal to the expected occupancy before invasion (Eq. **S6*A*** with $w' = 1$, $H_F = 1$, and $R' = 1$); the initial occupancy was therefore a vector of values of 0 and 1, with each element corresponding to a patch. We then began the simulation of colonization and extinction dynamics of each patch following Eq. **1**, with the vector p replaced by the vector of initial occupancies and using the vital rates and patch area of the postinvasion metapopulation; in other words, this was the onset of invasion in our simulations. Changes in occupancy for each patch (from occupied to empty or vice versa) were determined using Bernoulli trials with the probability given by Eq. **1*A***. We ran these simulations until the metapopulation went extinct or persisted for more than 2,000 generations. In Fig. 4*B* and Fig. S5, we report the time until all patches went extinct as the median time across the 150 simulations for a given combination of habitat loss and mean seed density.

Additional Parameters for Simulating Time to Extinction. The parameters c and e (Eq. **1** and Eq. **S6*A***) are not necessary for determining the change in metapopulation viability (Eq. **S6*B***), but they are necessary for simulating time to extinction when an extinction debt is present (Fig. 4*B*). We do not have direct estimates for these parameters, but reasonable estimates are available from our data, and we explored the effects of uncertainty in parameter estimation. Our estimates are based on scaling from our field-based results on individual seed success; these results give an indication of the number of seeds required to colonize successfully (informing our estimate of c) and the likelihood that a small number of seeds will go extinct without producing more offspring (i.e., the parameter e). Our estimates were generated as follows.

Let the seed germination rate be g, the survival rate of ungerminated seeds be s_u, the survival rate from germinated seed to plant be s_p, and the seed production of surviving plants be Poisson-distributed with mean m. The probability that a single seed will produce zero seeds in one generation is $g(1-s_p) + (1-g)(1-s_u) + e^{-m}$; the probability that it will produce one seed is $(1-g)\,s_u + me^{-m}$; the probability of producing n seeds, where $n > 1$, is the Poisson probability of n seeds multiplied by gs_p. Assuming no intraspecific density effects at the earliest stages of population growth, these probabilities can be used for multiple seeds while treating each

seed as independent; the total number of seeds in generation 2 is then equal to the sum produced by the individual seeds from generation 1. Our experiments provided direct measurements of g, s_p, and s_u. We combined these estimates from all species, giving mean values of $g = 0.16$, $s_p = 0.44$, and $s_u = 0.24$ (Table S5). In addition, we could solve numerically for m by assuming positive population growth rates, where the expected finite rate of increase E(R) is:

$$E(R) = mgs_p + (1-g)s_u. \quad \textbf{[S7]}$$

The parameter $1/c$ defines the half-saturation point of the colonization probability, meaning that when $1/c$ seeds arrive in a patch, there is a 50% chance of colonization. We ran simulations to determine the number of seeds required to reach a colonization probability of 0.5, where colonization was scored as a "fail" if the population reached zero and as a success if it reached 100 (again, assuming density independence in all cases). We found that for all finite rates of increase >2.2, which occurred with $m > 29$, this probability converged at the maximum $1/c = 7.85$. The estimate of $c = 0.127$ is therefore the maximum estimate possible with our data. At finite rates of increase below 2.2, the parameter c varied from 0.031 [$E(R) = 1.1$] to 0.111 [$E(R) = 2.2$].

The parameter e gives the probability that a population with a size of one will go extinct. For annual plants, we defined this as the probability that a population of size one would go extinct without producing a new viable seed (i.e., we assume that a seed that has survived in the seed bank cannot disperse to another patch but that its offspring can). The probability that at least one new seed will be produced is:

$$p(x \geq 1) = gs_p\left(1-e^{-1}\right)\sum_{i=0}\{(1-g)s_u\}^i = \frac{gs_p\left(1-e^{-1}\right)}{1-s_u(1-g)}. \quad \textbf{[S8]}$$

The parameter e is equal to 1 − Eq. **S8**, which is 0.944 for our data. The estimates for c and e that we used were based on an "average species," meaning that we averaged the germination and survival rates for all species. Because these estimates could presumably alter the time lines of an extinction debt (Fig. 4*B*), we reran these simulations with each parameter ± 0.1 but with maximum e set at 1 (i.e., the largest symmetrical differences possible while maintaining parameters within the bounds of 0–1). These simulations were used to determine the sensitivity of extinction time lines to the parameters c and e (Fig. S5). In some cases, this caused the extinction probability to be greater than 1 in some patches (i.e., in patches with $\mu * A_i < 1$); in such case, we used the convention that $E_i = min\ (1, E_i)$ (1, 3).

Focal Species and Habitat. We selected seven native annual species that occur on refugia and that are abundant enough to provide sufficient seed for our experiments: *Chaenactis galibriuscula*, *Chorizanthe palmerii*, *Lasthenia californica*, *Lotus wrangelianus*, *Micropus californicus*, *Plantago erecta*, and *Salvia columberiae*. We conducted field-based experiments and sampling in an area of ∼8 ha at the northern edge of the Sedgwick Reserve (34° 44' 20" North, 120° 01' 34" West) in Santa Barbara County, California. The area has a natural metapopulation structure, with refugia of annual native plants occurring on slightly raised mounds with coarse soils (9). The area between refugia is almost completely covered with exotic grasses, mainly *Avena fatua*, *Avena barbata*, and *Bromus* sp. Pockets of native bunchgrasses (mainly *Stipa pulchra*, *Stipa lepida*, and *Stipa cernua*) persist in small patches among these invasive grasses.

To develop the spatial metapopulation model, we surveyed refugia locations and areas within a 5.1-ha area of our study site (Sedgwick Reserve). This area, demarcated by a road on one side and natural boundaries (i.e., stream, different habitat types) on other sides, contained a total of 118 refugia. Refugia varied in size from 0.1 to 181 m^2 and covered a total of 5.5% of the surveyed area. Refugia were identified either through the presence of indicator native annual plants or as areas without native annuals but with similar characteristics (open, coarse-grained soils) and lacking dense invasive grasses. For model simplification, we calculated the centers and area of refugia and modeled them as circles on the landscape.

Field Experiments. ***Habitat quality experiment.*** Exotic grass invasion makes it difficult to determine the degree to which native species once performed in now invaded areas. Therefore, seed production rates in different portions of the landscape were estimated using an exotic grass competitor removal experiment, with 20 × 20-cm plots placed on refugia and at small distances from the refugia edge in the matrix. In all plots, all competitors were initially removed and the same density of native annual seed (3 g species^{-1}·m^{-2}) was sown. These densities were higher than those that are typically observed on refugia (5) to ensure that plants were in a competitive environment. All habitat quality plots were paired, with one plot used to estimate seed production and the other used to measure germination and seedling survival (to maturity) rates. A total of 96 plots were established.

Seed production for each pair of plots was estimated as the number of viable seeds produced, plus s_u (1–g), where g is the germination fraction and s_u is the survival rate of ungerminated seeds (5). The survival of ungerminated seeds (s_u) was estimated by testing their viability before and after a year of burial in nylon mesh bags (5). All seed production values were divided by mean seed production on refugia to give the ratio of the finite rates of increase in invaded areas relative to those on refugia (parameter v).

Significant differences in seed production between locations (i.e., refugia vs. matrix) were first tested using a nested distance-based permutation multivariate ANOVA (MANOVA) (10). Following a significant result, the ratio of seed production between habitats was tested for each species using generalized least squares (gls), which accounted for heterogeneous variances and the nested observations at each refugia. The gls results were confirmed by testing the number of viable seeds produced in each habitat using a generalized linear mixed model with a quasi-Poisson distribution and determining the ratio from the output of that model. These two approaches produced nearly identical results, and we therefore only report the results of the gls analyses. These and all other analyses were performed using R (11).

In each of the refugia that were used to conduct the habitat quality experiment, we also collected data from two 0.25-m^2 control quadrats (i.e., undisturbed quadrats). We calculated species richness in these combined quadrats, including our focal species and five other common refugia species. We calculated the area of each of these refugia and tested the correlation between refugia size and species richness per 0.5 m^2 to determine if larger refugia contained more species per unit area (Fig. S2), as predicted by theory (12).

Matrix permeability experiment. We estimated our focal species' finite rates of increase in the matrix (R) before and after invasion by sowing seeds into remnant native bunch grass locations and exotic annual grass locations. We first located remnant patches of native bunchgrass and placed paired plots in native bunchgrasses and in adjacent (<1.5-m distant) patches of invasive grass. Exotic grasses were weeded from between bunchgrass clumps and counted, and the same number of exotic grass stems was weeded at random from patches of invasive grasses.

Two plots were placed in each type of grass: full-density seeding, using the seed densities from natural refugia, and low-density seeding, with the latter used to determine if population growth rates differ when only small amounts of seed are present. These two treatments represent situations in which many or a few native seeds land among grasses. Finite rates of increase in low- and high-density plots did not differ significantly ($P > 0.05$ for all species), indicating

that species mainly experienced competition from surrounding grasses; thus, these estimates were combined for analysis. Finite rates of increase were determined as viable seeds produced/viable seeds added. These estimates assume that ungerminated seeds do not contribute to population growth, which is appropriate when seed germination is consistently close to zero, as was the case among the grasses. Because seeds in native bunchgrass plots were only sown between clumps, finite rates of increase in these plots were scaled by the proportion of each plot that was not occupied by bunchgrass bases (where native annuals cannot establish). A nested distance-based permutation MANOVA (10) was first used to test for significant differences between bunchgrass and exotic grasses. Following a significant result, individual tests were performed for each species with generalized linear mixed models using penalized quasilikelihood and a quasi-Poisson distribution.

Seed dispersal estimates. Seed dispersal rates were first estimated from well-established relationships between dispersal distances, plant height, and dispersal syndrome (13), and they were then validated. According to these relationships, mean dispersal distances for our species range from 0.1 to 0.5 m, with the lower estimate for the shortest plant with no dispersal mechanism and the higher estimate for the tallest of the wind-dispersed plants. When approximated using a normal (Gaussian) dispersal kernel, these dispersal distances correspond to rms dispersal distances (σ) of 0.25 to 0.63 m. We used two empirical methods to test the validity of these seed dispersal estimates. We created "false refugia" in 2008 by clearing circular, 50-m^2 areas of invasive grasses. These false refugia were placed across the study area, with nearest edges ranging from 0.5 to 7 m from the nearest refugia. Germinants of our focal species were counted in 2009, with this number likely overestimating colonization because it included any extant seed bank. In addition, in 2009, we chose two refugia that contained all species and placed seed traps (28 × 52 cm, 92 total seed traps) at up to 8 m from the refugia, with more traps placed at greater distances to account for the change in total area. Seed trap data could not be attained for *Lasthenia* due to small seed size or for *Lotus* because congeneric species made identification unreliable; for these taxa, we were restricted to using colonization rates on false refugia.

Very low colonization rates of false refugia and an almost complete lack of seed dispersal into seed traps (Table S4) indicate that our species were as dispersal-limited as predicted from relationships established in the literature. For example, *Plantago* is one of the most abundant species on refugia, with ∼730 seeds per square meter. Only two *Plantago* plants were found on the 11 false refugia placed on the landscape, even though these false refugia each had an area of 50 m^2 and were placed from 0.5 to 7 m from occupied refugia. *Plantago* had a greater colonization rate than four other species on the false refugia and a lower rate than two species (Table S4). Likewise, a total of 10 seeds were found in seed traps between 0 and 2 m from the refugia edge; when correcting for area sampled, ∼2.5% of *Plantago* seeds disperse between 0.1 m and 2 m from the patch edge. Compared with the dispersal of a plant with an rms dispersal distance of 1 m, *Plantago* had about one-sixth the proportion of seeds expected. Because metapopulation models are sensitive to assumptions about dispersal, we chose to use this large estimate of seed dispersal (i.e., $\sigma = 1$ m) in all the tests presented in the main text to represent the most conservative scenario for the development of an extinction debt. We also generate estimates assuming an rms dispersal distances (σ) of 0.5 m to generate a range of estimates (Figs. S2 and S3). We chose to alter mean dispersal distances instead of the shape of the kernel both for logistical reasons and because the model was more sensitive to mean distance (*Model assumptions*).

1. Ovaskainen O, Hanski I (2001) Spatially structured metapopulation models: Global and local assessment of metapopulation capacity. *Theor Popul Biol* 60(4):281–302.
2. Hanski I, Ovaskainen O (2000) The metapopulation capacity of a fragmented landscape. *Nature* 404(6779):755–758.
3. Hanski I (1994) A practical model of metapopulation dynamics. *J Anim Ecol* 63(1): 151–162.
4. Hanski I (1994) Patch-occupancy dynamics in fragmented landscapes. *Trends Ecol Evol* 9(4):131–135.
5. Levine JM, HilleRisLambers J (2009) The importance of niches for the maintenance of species diversity. *Nature* 461(7261):254–257.
6. Turchin P (1998) *Quantitative Analysis of Movement: Measuring and Modeling Population Redistribution in Animals and Plants* (Sinauer Associates, Sunderland, MA).
7. Muller-Landau HC, Wright SJ, Calderón O, Condit R (2008) Interspecific variation in primary seed dispersal in a tropical forest. *J Ecol* 96(4):653–667.
8. Hanski I (1998) Metapopulation dynamics. *Nature* 396(6706):41–49.
9. Gram WK, et al. (2004) Distribution of plants in a California serpentine grassland: Are rocky hummocks spatial refuges for native species? *Plant Ecol* 172(2):159–171.
10. McArdle B, Anderson M (2001) Fitting multivariate models to community data: A comment on distance-based redundancy analysis. *Ecology* 82(1):290–297.
11. R Development Core Team (2011) *R: A Language and Environment for Statistical Computing* (R Foundation for Statistical Computing, Vienna).
12. Holt RD (1993) *Species Diversity in Ecological Communities*, eds Ricklefs RE, Schluter D (Univ of Chicago Press, Chicago), pp 77–88.
13. Thomson FJ, Moles AT, Auld TD, Kingsford RT (2011) Seed dispersal distance is more strongly correlated with plant height than with seed mass. *J Ecol* 99(6):1299–1307.

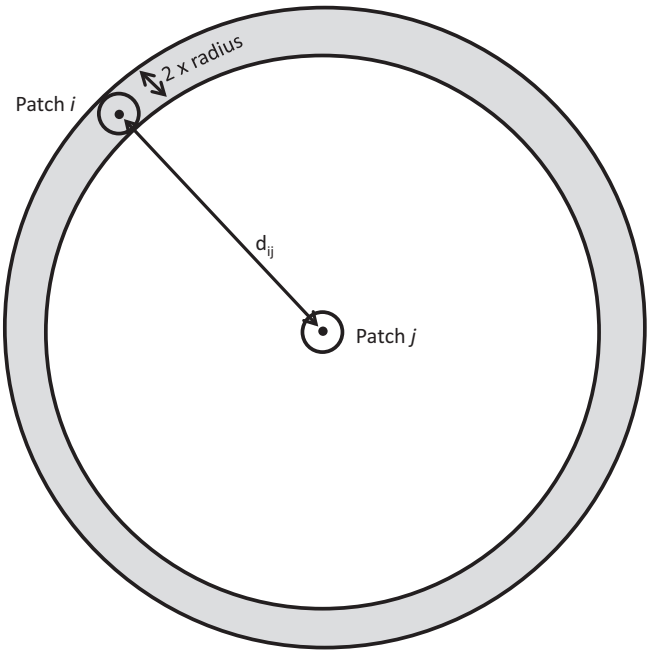

Fig. S1. Effect of the receiver patch area on the probability of seed recruitment. The seed must disperse between the distance $d_{ij} \pm radius_i$. Seeds that disperse that distance arrive at the focal patch with a probability equal to $\frac{A_i}{\pi(d_{ij}+radius_i)^2-\pi(d_{ij}-radius_i)^2}=\frac{radius_i}{4d_{ij}}$.

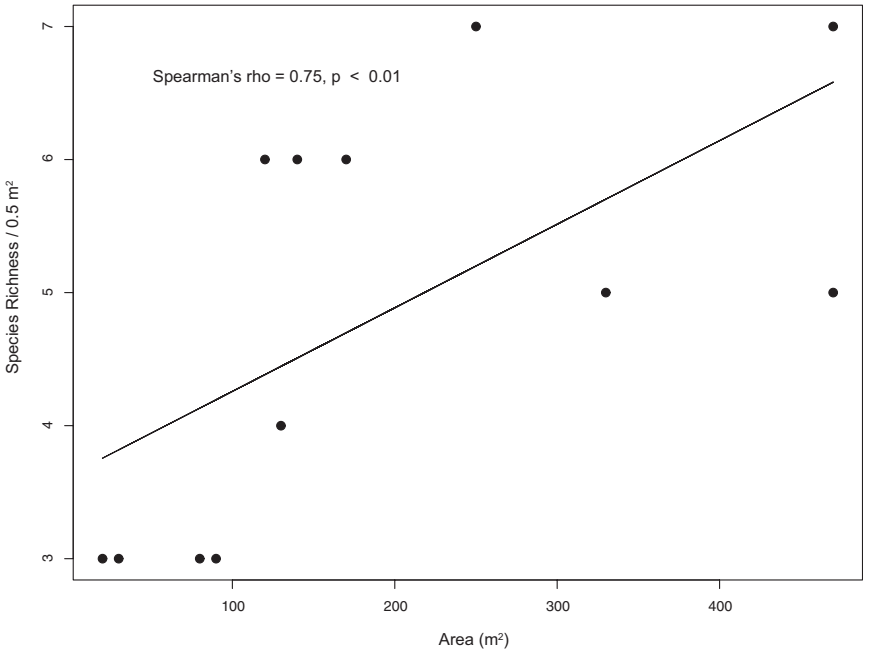

Fig. S2. Species richness in a fixed sampling area (0.5 m^2) increases significantly with the total area of the refugia. This positive trend is predicted by metapopulation theory (12), which posits that larger patches should accumulate more species per unit area because of their greater colonization-to-extinction rate ratios. Although this pattern is correlational and need not reflect metapopulation mechanisms, most factors that covary with patch area, such as increased environmental heterogeneity in larger patches (at a scale larger than our 0.5-m^2 sampling plots), do not predict an increase in richness per unit area.

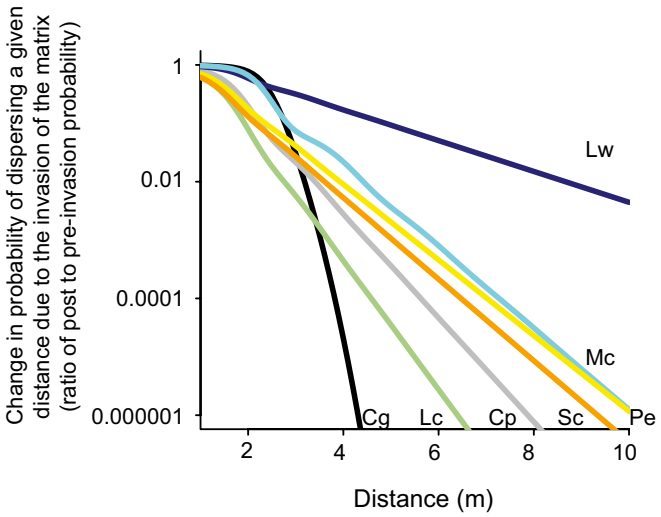

Fig. S3. Ratio of colonization probability postinvasion to preinvasion due to invasion of the matrix when the rms dispersal distance (σ) is 0.5 m. Expected colonization was estimated from Eq. **S5**, with the summation calculated over 30 generations. Colors and species labels are as in Fig. 2*C*.

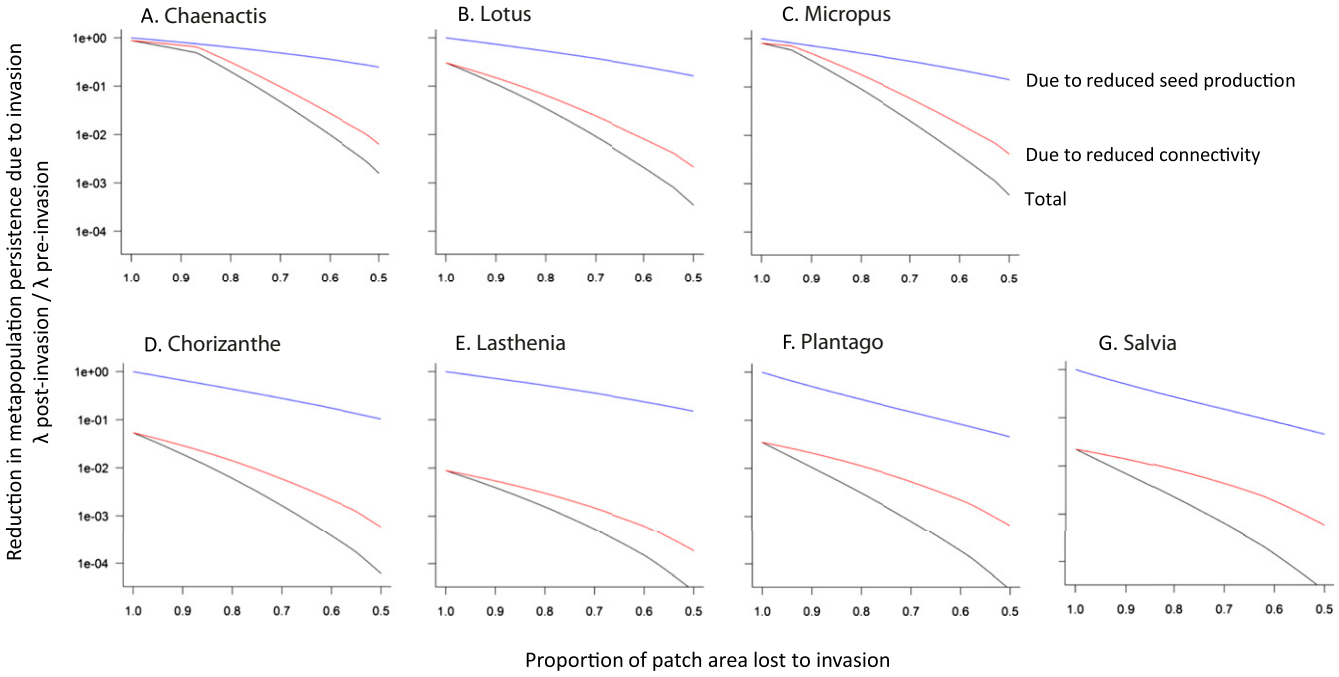

Fig. S4. Reduction in metapopulation viability following invasion for each species with an rms dispersal distance (σ) of 0.5 m. The change in viability (*y* axis) is the ratio of the leading eigenvalue of the metapopulation postinvasion to preinvasion, and it is further explained in *SI Materials and Methods*. Panels correspond to the species listed by genus name (full names are given in Fig. 2).

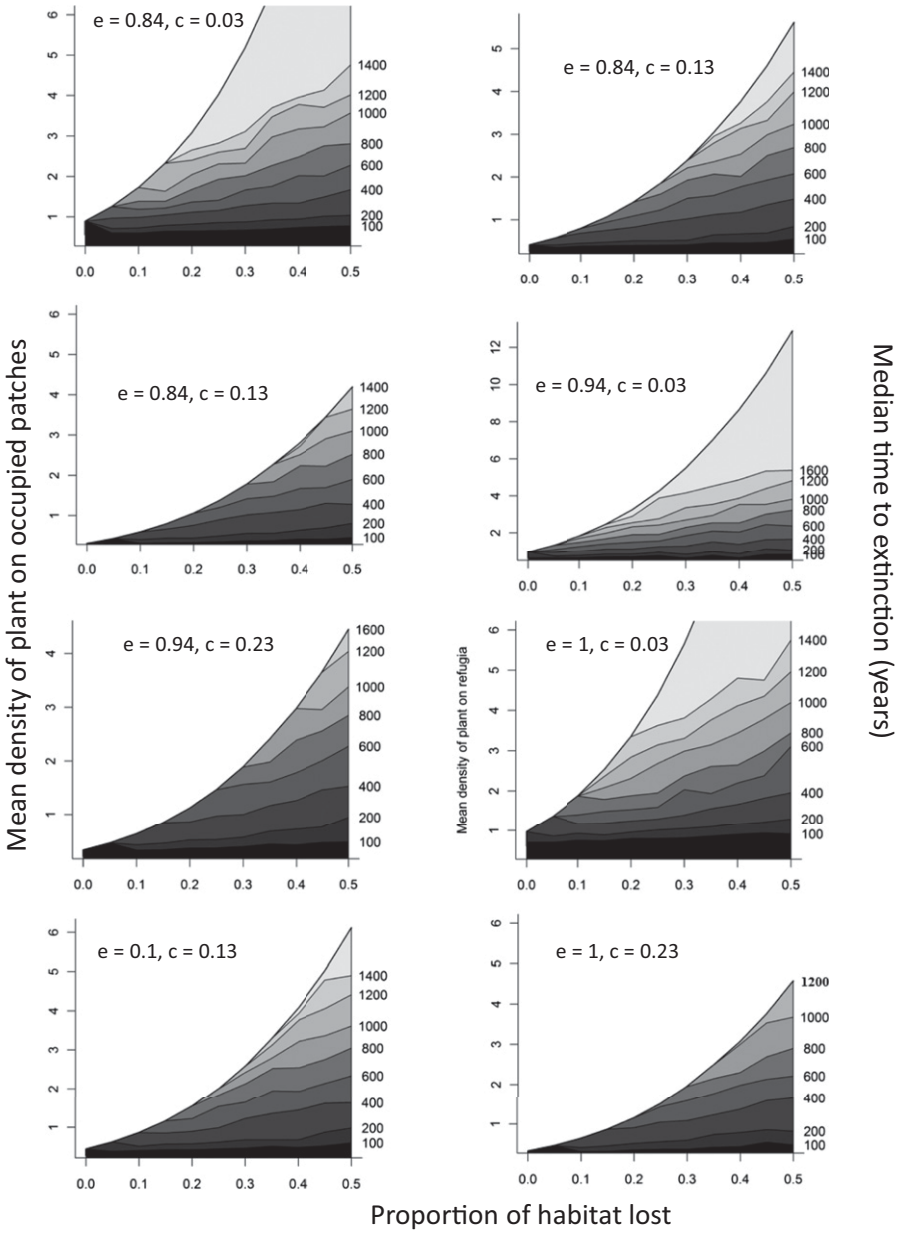

Fig. S5. Median time to extinction for an average species with a given mean density and proportion of habitat loss. The sensitivity of extinction debt time lines to changes in two of the estimated parameters, *e* and *c*, is shown. Variation in these parameters causes slight changes in the range of densities at which an extinction debt arises (*y* axis to the left); however, in all parameter ranges, extinction debts often persist for 200–800 y after invasion. Each panel is based on 24,200 simulations using the parameters stated, along with parameters averaged for all species.

Table S1. Relative finite rates of increase in refugia and invaded areas at the edge of refugia

Species	Relative finite rate of increase		
	Refugia	Invaded area	Invaded/refugia
Chaenactis glabriuscula (Cg)	0.96 (0.07)	1.05 (0.09)	1[†]
Chorizanthe palmerii (Cp)	1.09 (0.37)	2.27 (0.44)**	2.10
Lasthenia californica (Lc)	1.17 (0.15)	1.83 (0.18)***	1.57
Lotus wrangelianus (Lw)	1.00 (0.20)	1.48 (0.26)[+]	1.47
Micropus californicus (Mc)	1.03 (0.20)	1.70 (0.24)**	1.65
Plantago erecta (Pe)	0.92 (0.40)	3.39 (0.62)***	3.68
Salvia columbariae (Sc)	0.98 (0.39)	3.64 (0.46)***	3.70

[+]$P < 0.1$; *$P < 0.05$; **$P < 0.01$, ***$P < 0.001$; tests if value is significantly different in refugia.
[†]Set to 1 because of nonsignificant difference between refugia and invaded areas. These data were incorporated into Eqs. **4** and **S6** through the relative quality of the refugia before and after invasion, w'. $w' = \frac{1}{H_F(1-v)+v}$ where H_f is the fraction of patch habitat eliminated by invasion and v is the finite rate of increase in invaded areas/refugia (fourth column in table).

Table S2. Finite rates of increase in matrix areas among native bunchgrasses and exotic grasses

Species	Finite rate of increase (R) among*				P
	Exotic grasses		Native bunchgrass		
Chaenactis glabriuscula (Cg)	0.00		0.01	(0.004–0.030)	NA[†]
Chorizanthe palmerii (Cp)	0.01	(0.006–0.021)	0.14	(0.113–0.180)	0.003
Lasthenia californica (Lc)	0.02	(0.011–0.026)	0.28	(0.199–0.399)	<0.001
Lotus wrangelianus (Lw)	0.04	(0.019–0.070)	0.08	(0.043–0.135)	0.279
Micropus californicus (Mc)	0.002	(0.001–0.003)	0.02	(0.012–0.036)	0.002
Plantago erecta (Pe)	0.06	(0.027–0.113)	0.25	(0.187–0.342)	0.062
Salvia columbariae (Sc)	0.07	(0.042–0.133)	0.34	(0.254–0.448)	0.029

Values in parentheses give the mean ± SE. P values are from species-specific generalized linear mixed models using penalized quasilikelihood and a quasi-Poisson distribution to test if the two grass types differed significantly.
*Estimates for each grass type (exotic vs. native) were used in model predictions for all species (Figs. 2*C* and 3 and Figs. S2 and S3).
[†]Could not be tested because *Chaenactis* did not produce seeds when grown in exotic grass patches.

Table S3. Parameters included in model and sources for parameter estimates

Parameter	Explanation	Source of estimate
Models S5 and S6*B*	Model S5: matrix permeability Model S6*B*: change in metapopulation viability	
w'	Ratio of seed density postinvasion to preinvasion; determined from the habitat fraction (H_F) and the ratio of finite rates of increase on habitat lost to invaders and habitat remaining postinvasion (υ; see explanation for Eq. **S6*B***).	Habitat quality experiment. Results for υ are given in Fig. 2*A* and Table S1.
H_F	Fraction of native annual habitat remaining after invasion	This parameter is not empirically estimated. We calculate all impacts over an H_F ranging from 1 (no habitat loss) to 0.5 (50% habitat loss).
R	Native annual population growth rate in matrix among native bunchgrasses	Matrix permeability experiment. Results are given in Fig. 2*B* and Table S2.
R'	Native annual population growth rate in matrix among exotic grasses	Matrix permeability experiment. Results are given in Fig. 2*B* and Table S2.
σ	Rms dispersal distance	Dispersal estimated from published sources and two sampling experiments. Due to uncertainty in this parameter, all impacts were calculated for estimated dispersal distances and greater dispersal distances ($\sigma = 0.5$ m in Fig. S3 and $\sigma = 1$ in Fig. 3, respectively). Results in all main figures were produced with the larger dispersal distance to generate a conservative impact of fragmentation.
Simulation of times to extinction	These simulations required the parameters listed above, plus the following	
c	Determines the rate at which the probability of colonization increases as more seeds arrive. In particular, the number of seeds required for a 50% probability of colonization is 1/c.	Estimated with data from the habitat quality experiment (*SI Materials and Methods, Additional Parameters for Simulating Time to Extinction*). Because this estimate may vary from year to year, and our uncertainty in its component vital rates, we reran simulations with c ranging symmetrically around this estimate.
e	Per-individual extinction rate	Estimated with data from the habitat quality experiment. (*SI Materials and Methods, Additional Parameters for Simulating Time to Extinction*). Because this estimate may vary from year to year, and our uncertainty in its component vital rates, we reran simulations with e ranging symmetrically around this estimate.
μ	Average density of the focal species (individuals m^{-2}) within patches	This parameter was varied in simulations (y axis on left for Fig. 4 and Fig. S4) to assess the sensitivity of extinction to mean local abundance.

Table S4. Seed dispersal results from seed traps and false refugia

Species	No. of seeds in traps <2 m from refugia edge*	Density (seeds m^{-2}) on nearby refugia, $\mu^{\dagger}$	Total no. of "false refugia" colonized‡
Chaenactis glabriuscula (Cg)	0	343	0
Chorizanthe palmerii (Cp)	0	431	1
Lasthenia californica (Lc)	—	6,290	7
Lotus wrangelianus (Lw)	—	137	6
Micropus californicus (Mc)	0	218	0
Plantago erecta (Pe)	10	704	2
Salvia columbariae (Sc)	0	878	0

*Fifty-five seed traps for a total coverage of ~7.5 m^2. Traps were placed to be more numerous at larger distances such that ~13% of the total area between 0 and 2 m from refugia was covered with seed traps. Species marked "—" had seeds that were too small to reliably find (Lc) or had multiple congeners with similar seeds (Lw).

†Estimates of density were obtained from the habitat quality experiment.

‡Eleven false refugia were created by clearing 50 m^2 of invasive grasses at 11 locations ranging in distance from 0.5 to 7 m from the nearest refugia.

Table S5. Parameter estimates for each species studied

Species	Ungerminated seed survival, s_u	Seed germination, g	Germinant survival to reproduction, s_p
Chaenactis glabriuscula (Cg)	0.12	0.14	0.15
Chorizanthe palmerii (Cp)	0.15	0.15	0.37
Lasthenia californica (Lc)	0.20	0.12	0.50
Lotus wrangelianus (Lw)	0.13	0.04	0.08
Micropus californicus (Mc)	0.09	0.04	0.50
Plantago erecta (Pe)	0.66	0.36	0.50
Salvia columbariae (Sc)	0.34	0.29	0.49

Two parameters (s_u and g) were used to determine the finite rate of increase of species in refugia and invaded areas (Fig. 2*A*), and the average of these rates across species were used in simulations of times to extinction (Fig. 4 and Fig. S4). These, along with germinant survival to reproduction, s_p, were also used to estimate c and e for simulations of times to extinction (*SI Materials and Methods, Additional Parameters for Simulating Time to Extinction*). Estimates for parameters g and s_p were obtained from the habitat quality experiment, whereas the estimate for s_u was obtained from seeds that were buried in mesh bags over one growing season.